Chapter 16

16.1

The difference between systems A and B lies in the dynamic lag in the measurement elements G_{m1} (primary loop) and G_{m2}(secondary loop). With a faster measurement device in A, better control action is achieved. In addition, for a cascade control system to function properly, the response of the secondary control loop should be faster than the primary loop. Hence System A should be faster and yield better closed-loop performance than B.

Because G_{m2} in system B has an appreciable lag, cascade control has the potential to improve the overall closed-loop performance more than for system A. Little improvement in system A can be achieved by cascade control versus conventional feedback.

Comparisons are shown in Figs. S16.1a/b. PI controllers are used in the outer loop. The PI controllers for both System A and System B are designed based on Table 12.1 (τ_c = 3). P controllers are used in the inner loops. Because of different dynamics the proportional controller gain of System B is about one-fourth as large as the controller gain of System A

System A: K_{c2} = 1 K_{c1}=0.5 τ_I=15
System B: K_{c2} = 0.25 K_{c1}=2.5 τ_I=15

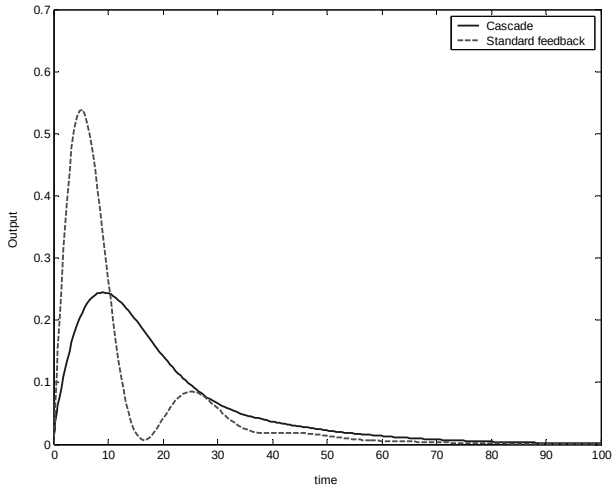

Figure S16.1a. *System A. Comparison of D_2 responses (D_2=1/s) for cascade control and conventional PI control.*

In comparing the two figures, it appears that the standard feedback results are essentially the same, but the cascade response for system A is much faster and has much less absolute error than for the cascade control of B

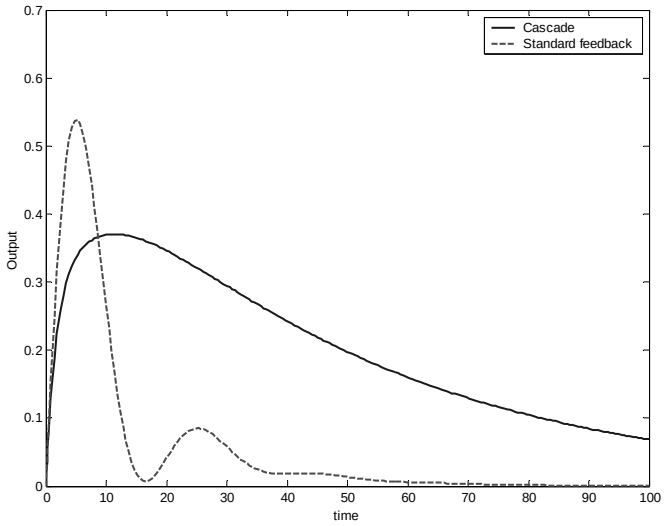

Figure S16.1b. *System B .Comparison of D_2 responses (D_2=1/s) for cascade control and conventional PI control.*

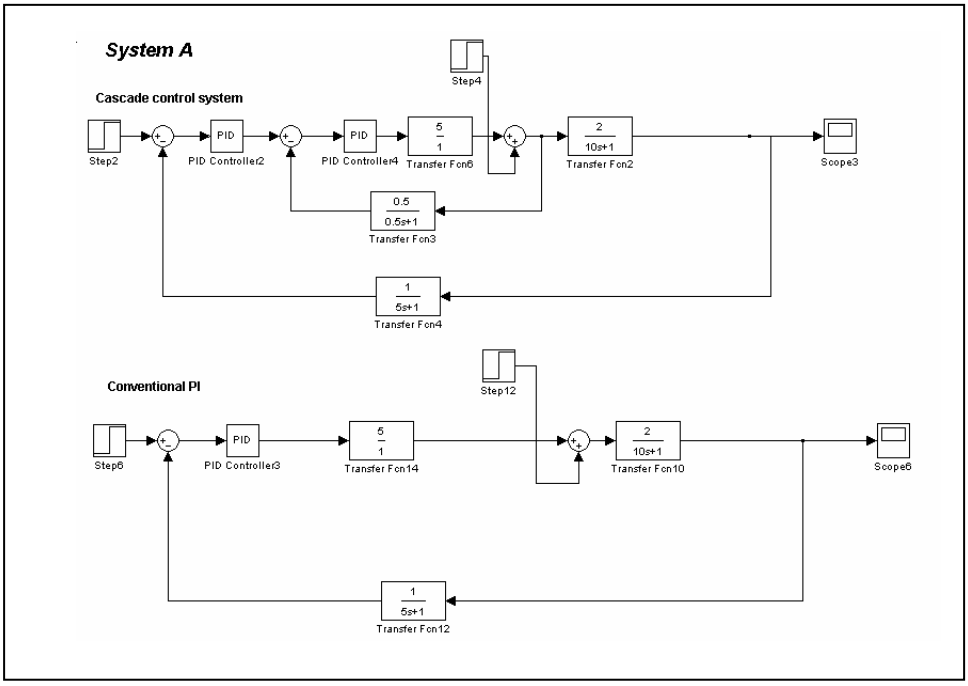

Figure S16.1c. *Block diagram for System A*

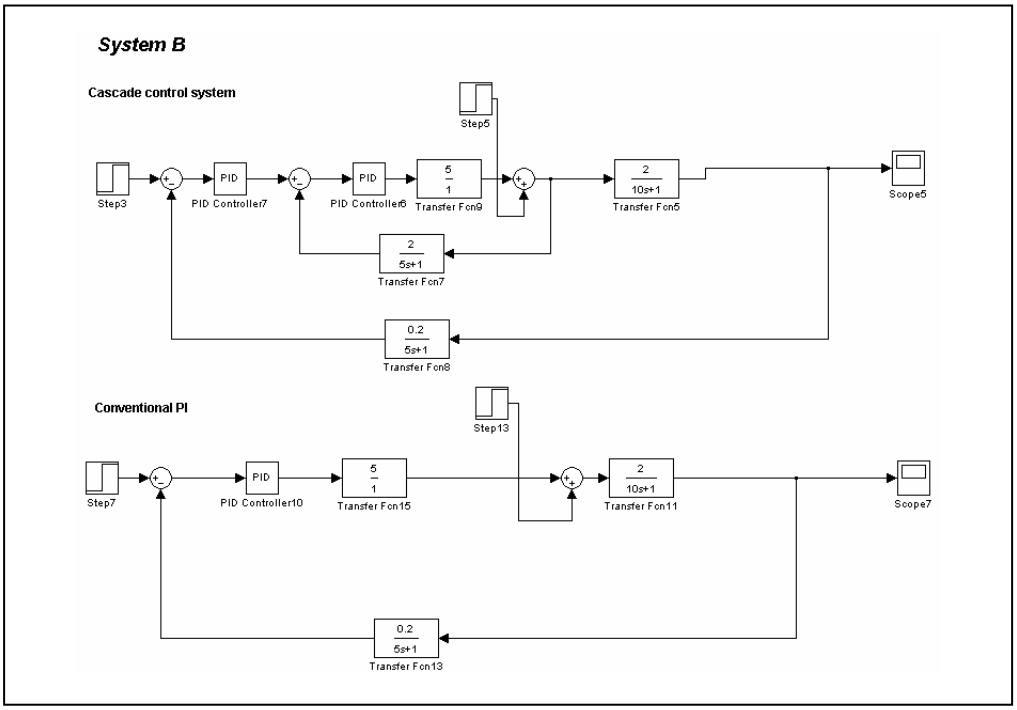

Figure S16.1d. *Block diagram for System B*

16.2

a) The transfer function between Y_1 and D_1 is

$$\frac{Y_1}{D_1} = \frac{G_{d1}}{1 + G_{c1}\left(\frac{G_{c2}G_v}{1 + G_{c2}G_vG_{m2}}\right)G_pG_{m1}}$$

and that between Y_1 and D_2 is

$$\frac{Y_1}{D_2} = \frac{G_pG_{d2}}{1 + G_{c2}G_vG_{m2} + G_{c2}G_vG_{m1}G_{c1}G_p}$$

using $G_v = \dfrac{5}{s+1}$, $G_{d2} = 1$, $G_{d1} = \dfrac{1}{3s+1}$,

$$G_p = \frac{4}{(2s+1)(4s+1)} \ , \ G_{m1} = 0.05 \ , \quad G_{m2} = 0.2$$

For $G_{c1} = K_{c1}$ and $G_{c2} = K_{c2}$, we obtain

$$\frac{Y_1}{D_1} = \frac{8s^3 + (14 + 8K_{c2})s^2 + (7 + 6K_{c2})s + K_{c2} + 1}{24s^4 + (50 + 24K_{c2})s^3 + [10 + K_{c2}(9 + 3K_{c1})]s + (35 + 26K_{c2})s^2 + K_{c2}(1 + K_{c1}) + 1}$$

$$\frac{Y_1}{D_2} = \frac{4(s+1)}{8s^3 + (14 + 8K_{c2})s^2 + (7 + 6K_{c2})s + K_{c2}(1 + K_{c1}) + 1}$$

The figures below show the step load responses for K_{c1}=43.3 and for K_{c2}=25. Note that both responses are stable. You should recall that the critical gain for K_{c2}=5 is K_{c1}=43.3. Increasing K_{c2} stabilizes the controller, as is predicted.

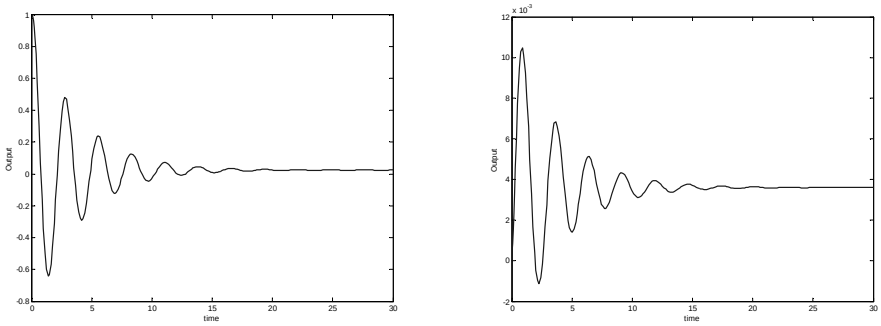

Figure S16.2a. *Responses for unit load change in D_1 (left) and D_2 (right)*

b) The characteristic equation for this system is

$$1 + G_{c2}G_vG_{m2} + G_{c2}G_vG_{m1}G_{c1}G_p = 0 \qquad (1)$$

Let $G_{c1}=K_{c2}$ and $G_{c2}=K_{c2}$. Then, substituting all the transfer functions into (1), we obtain

$$8s^3 + (14 + 8K_{c2})s^2 + (7 + 6K_{c2})s + K_{c2}(1 + K_{c1}) + 1 \qquad (2)$$

Now we can use the Routh stability criterion. The Routh array is

Row 1	8	$7 + 6K_{c2}$
Row 2	$14 + 8K_{c2}$	$1 + K_{c2}(1 + K_{c1})$
Row 3	$\dfrac{24K_{c2}^{\ 2} + 66K_{c2} + 45 - 4K_{c1}K_{c2}}{7 + 4K_{c2}}$	0
Row 4	$1 + K_{c2}(1 + K_{c1})$	

For $1 \le K_{c2} \le 20$, there is no impact on stability by the term $14+8K_{c2}$ in the second row. The critical K_{c1} is found by varying K_{c2} from 1 to 20, and using

$$24K_{c2}^{\ 2} + 66K_{c2} + 45 - 4K_{c1}K_{c2} \ge 0 \quad (3)$$

$$1 + K_{c2}(1 + K_{c1}) \ge 0 \quad (4)$$

Rearranging (3) and (4), we obtain

$$K_{c1} \le \frac{24K_{c2}^{\ 2} + 66K_{c2} + 45}{4K_{c2}} \quad (5)$$

$$K_{c1} \ge -\left(\frac{K_{c2}+1}{K_{c2}}\right) \quad (6)$$

Hence, for normal (positive) values of K_{c1} and K_{c2},

$$K_{c1,u} = \frac{24K_{c2}^{\ 2} + 66K_{c2} + 45}{4K_{c2}}$$

The results are shown in the table and figure below. Note the nearly linear variation of K_{c1} ultimate with K_{c2}. This is because the right hand side is very nearly 6 K_{c2}+16.5. For larger values of K_{c2}, the stability margin on K_{c1} is higher. There don't appear to be any nonlinear effects of K_{c2} on K_{c1}, especially at high K_{c2}.

There is no theoretical upper limit for K_{c2}, except that large values may cause the valve to saturate for small set-point or load changes.

K_{c2}	$K_{c1,u}$
1	33.75
2	34.13
3	38.25
4	43.31
5	48.75
6	54.38
7	60.11
8	65.91
9	71.75
10	77.63
11	83.52
12	89.44
13	95.37
14	101.30
15	107.25
16	113.20
17	119.16
18	125.13
19	131.09
20	137.06

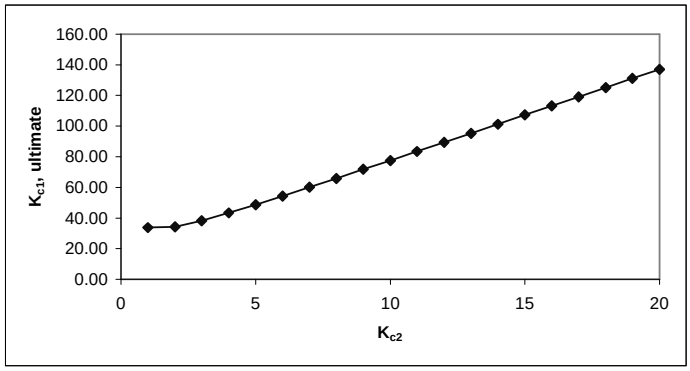

Figure S16.2b. *Effect of K_{c2} on the critical gain of K_{c1}*

c) With integral action in the inner loop,

$$G_{c1} = K_{c1}$$

$$G_{c2} = 5\left(1+\frac{1}{5s}\right)$$

Substitution of all the transfer functions into the characteristic equation yields

$$1+5\left(1+\frac{1}{5s}\right)\frac{5}{s+1}(0.2)+5\left(1+\frac{1}{5s}\right)\frac{5}{s+1}(0.05)K_{c1}$$

$$\frac{4}{(4s+1)(2s+1)} = 0$$

Rearrangement gives

$$8s^4 + 54s^3 + 45s^2 + (12+5K_{c1})s + K_{c1} + 1 = 0$$

The Routh array is:

Row 1	8	45	$1+K_{c1}$
Row 2	54	$12+5K_{c1}$	0
Row 3	$\frac{1167-20K_{c1}}{27}$	$1+K_{c1}$	
Row 4	$\frac{-100K_{c1}{}^2+4137K_{c1}+12546}{1167-20K_{c1}}$	0	
Row 5	$1+K_{c1}$		

Using the Routh array analysis

Row 3: $1167-20K_{c1} > 0 \quad \therefore \quad K_{c1} < 58.35$

$1+K_{c1} > 0 \quad \therefore \quad K_{c1} > -1$

Row 4: Since $1167-20K_{c1}$ is already positive,

$-100K_{c1}{}^2 + 4137K_{c1} + 12546 > 0$

Solving for the positive root, we get $K_{c1} < 43.3$

The ultimate K_{c1} is 43.3, which is the same result as for proportional only control of the secondary loop.

With integral action in the outer loop only,

$$G_{c1} = K_{c1}\left(1+\frac{1}{5s}\right)$$
$$G_{c2} = 5$$

Substituting the transfer functions into the characteristic equation.

$$1+5\frac{5}{s+1}(0.2)+5\frac{5}{s+1}(0.05)K_{c1}\left(1+\frac{1}{5s}\right)\frac{4}{(4s+1)(2s+1)}=0$$

$$\therefore\ 8s^4+54s^3+37s^2+(6+5K_{c1})s+K_{c1}=0$$

The Routh array is

Row 1	8	37	K_{c1}
Row 2	54	$6+5K_{c1}$	0
Row 3	$\frac{975-20K_{c1}}{27}$	K_{c1}	
Row 4	$\frac{-100K_{c1}^{\ 2}+3297K_{c1}+5850}{975-20K_{c1}}$	0	
Row 5	K_{c1}		

Using the Routh array analysis,

Row 3: $975-20>0$ $\quad\therefore\quad$ $K_{c1}<48.75$
$K_{c1}>0$

Row 4: Since $975-20K_{c1}$ is already positive,
$-100K_{c1}^{\ 2}+3297K_{c1}+5850>0$
Solving for the positive root, we get $K_{c1}<34.66$

Hence, K_{c1}<34.66 is the limiting constraint. Note that due to integral action in the primary loop, the ultimate controller gain is reduced.

Calculation of offset:

For $G_{c1} = K_{c1}\left(1+\frac{1}{\tau_{I1}s}\right)$, $G_{c2} = K_{c2}$, $(\tau_{I2} = \infty)$

$$\frac{Y_1}{D_1} = \frac{G_{d1}(1+K_{c2}G_vG_{m2})}{1+K_{c2}G_vG_{m2}+K_{c2}G_vG_{m1}K_{c1}\left(1+\frac{1}{\tau_{I1}s}\right)G_p}$$

$$\frac{Y_1}{D_1}(s=0) = 0$$

Since G_{c1} contains integral action, a step-change in D_1 does not produce an offset in Y_1.

$$\frac{Y_1}{D_2} = \frac{G_pG_{d2}}{1+K_{c2}G_vG_{m2}+K_{c2}G_vG_{m1}K_{c1}\left(1+\frac{1}{\tau_{I1}s}\right)G_p}$$

$$\frac{Y_1}{D_2}(s=0) = 0$$

Thus, for the same reason as before, a step-change in D_2 does not produce an offset in Y_1.

For $G_{c1} = K_{c1}$ (ie. $\tau_{I1} = \infty$) , $G_{c2} = K_{c2}\left(1+\frac{1}{\tau_{I2}s}\right)$

$$\frac{Y_1}{D_1} = \frac{G_{d1}(1+K_{c2}\left(1+\frac{1}{\tau_{I2}s}\right)G_vG_{m2})}{1+K_{c2}\left(1+\frac{1}{\tau_{I2}s}\right)G_vG_{m2}+K_{c2}G_vG_{m1}K_{c1}\left(1+\frac{1}{\tau_{I2}s}\right)G_p}$$

$$\frac{Y_1}{D_1}(s=0) \neq 0$$

Therefore, when there is no integral action in the outer loop, a primary disturbance produces an offset.

Thus, there is no offset for a step-change in the secondary disturbance.

.

$$\frac{Y_1}{D_2} = \frac{G_p G_{d2}}{1 + K_{c2}\left(1 + \frac{1}{\tau_{I2} s}\right) G_v G_{m2} + K_{c2} G_v G_{m1} K_{c1}\left(1 + \frac{1}{\tau_{I2} s}\right) G_p}$$

$$\frac{Y_1}{D_2}(s = 0) = 0$$

Thus, there is no offset for a step-change in the secondary disturbance.

16.3

a) Tuning the slave loop:

The open-loop transfer function is

$$G(s) = \frac{K_{c2}}{(2s+1)(5s+1)(s+1)}$$

Since a proportional controller is used, a high K_{c2} reduces the steady-state offset. The highest K_{c2} which satisfies the bounds on the gain and phase margins is 5.3. For this K_{c2}, the gain margin is 2.38, and the phase margin is 30.7°.

By using MATLAB, the Bode plot of $G(s)$ with K_{c2} = 5.3 is shown below.

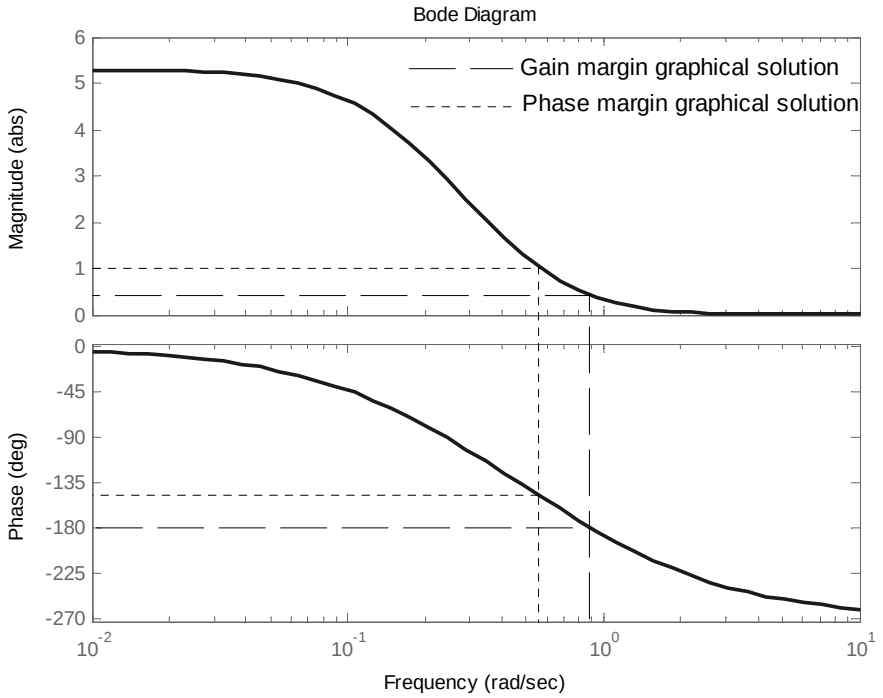

Figure S16.3a. *Bode plot for the inner open-loop; gain and phase margins.*

b) Tuning the master loop:

The input-output transfer function of the inner loop is

$$G_{in}(s) = \frac{5.3(s+1)}{10s^3 + 17s^2 + 8s + 6.3} \qquad \text{(with } K_{c2} = 5.3\text{)}$$

The ultimate gain $K_{c1,u}$ can be found by simulation. In doing so,

$K_{c1,u} = 3.2491$

The corresponding period of oscillation is

$P_u = 2\pi/\omega = 8.98$ time units.

The Ziegler-Nichols tuning criteria for a PI-controller yield

$K_{c1} = K_{c1,u} / 2.2 = 1.48$

$\tau_{I1} = P_u / 1.2 = 7.48$

The closed-loop response with these tuning constant values (K_{c1}=1.48, τ_{I1} = 7.48 , K_{c2} = 5.3) is shown below.

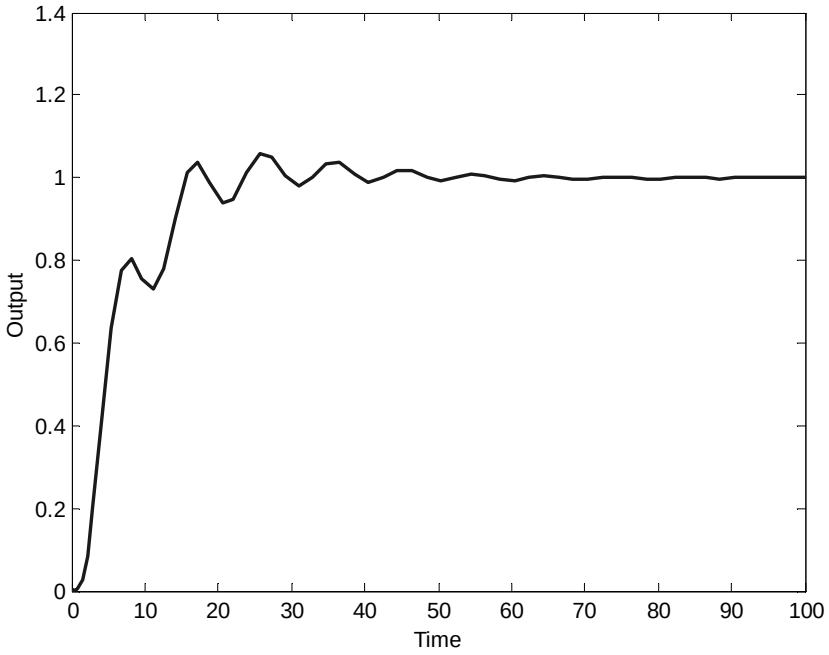

Fig S16.3b. *Closed-loop response for a unit step set-point change.*

16.4

For the inner controller (Slave controller), IMC tuning rules are used

$$G_{c2}^{*} = \frac{1}{G_2^{-}} = \frac{(2s+1)(5s+1)(s+1)}{(\tau_{c2}s+1)^3}$$

Closed-loop responses for different values of τ_{c2} are shown below. A τ_{c2} value of 3 yields a good response.

For the Master controller,

$$G_{c1}^{*} = \frac{1}{G_1^{-}} \qquad \text{where} \qquad G_1^{-} = \frac{(2s+1)(5s+1)(s+1)}{(\tau_{c1}s+1)^3}\frac{1}{(10s+1)}$$

This higher-order transfer function is approximated by first order plus time delay using a step test:

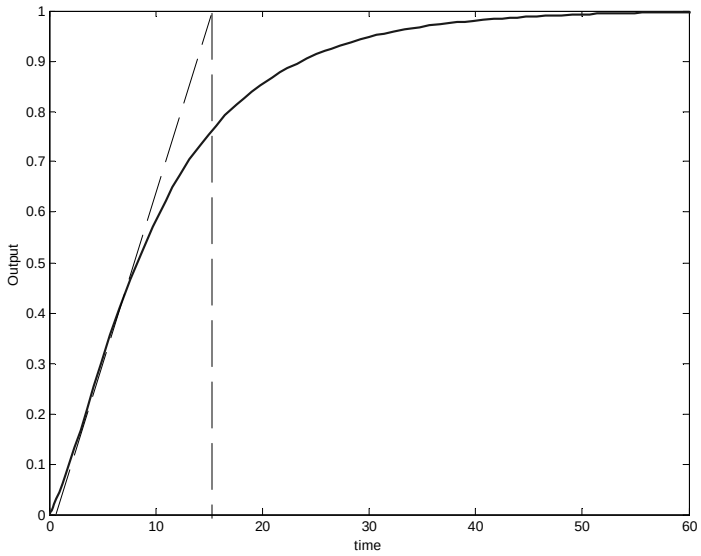

Figure S16.4. *Reaction curve for the higher order transfer function*

Hence $G_1^{-} \approx \dfrac{e^{-0.38s}}{(15.32s+1)}$

From Table 12.1: (PI controller, Case G): $K_c = \dfrac{15.32}{\tau_{c1}+0.38}$ and $\tau_i = 15.32$

Closed-loop responses are shown for different values of τ_{c1}. A τ_{c1} value of 7 yields a good response.

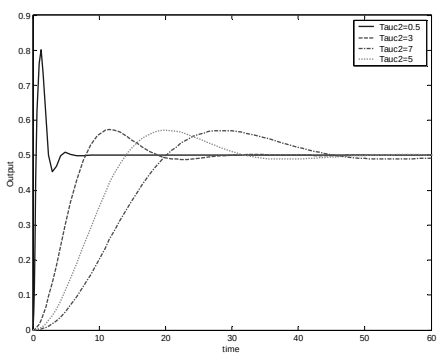

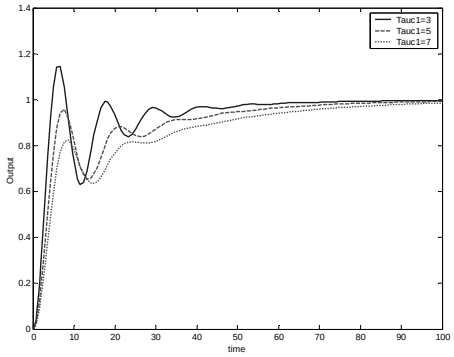

Figure S16.4b. Closed-loop response for τ_{c2} **Figure S16.4c**. Closed-loop response for τ_{c1}

Hence for the master controller, $K_c = 2.07$ and $\tau_I = 15.32$

16.5

a) The T_2 controller (TC-2) adjusts the set-point, T_{1sp}, of the T_1 controller (TC-1). Its output signal is added to the output of the feedforward controller.

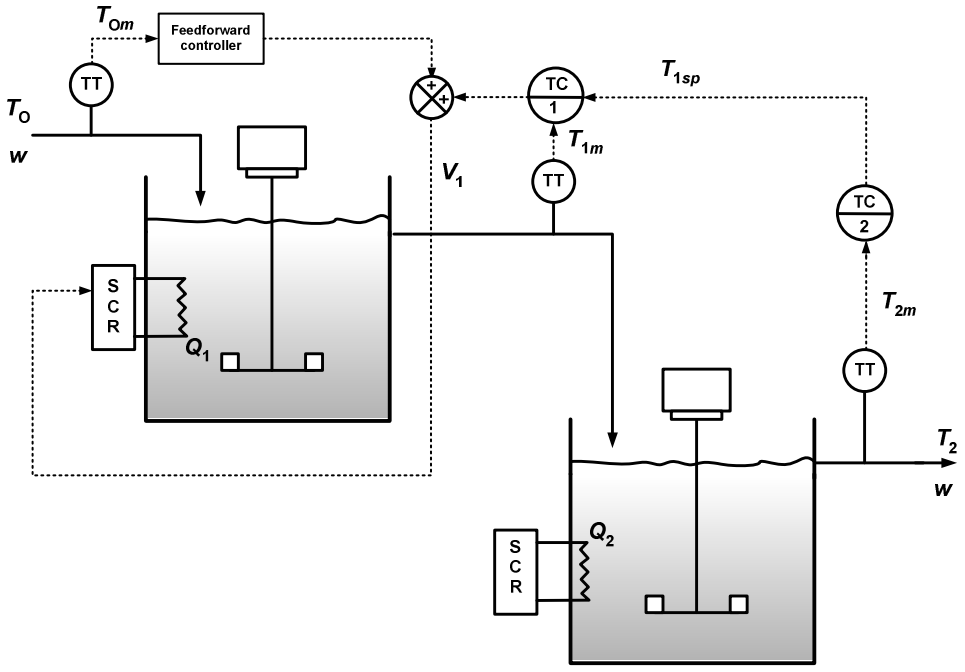

Figure S16.5a. *Schematic diagram for the control system*

b) This is a cascade control system with a feedforward controller being used to help control T_1. Note that T_1 is an intermediate variable rather than a disturbance variable since it is affected by V_1.

c) Block diagram:

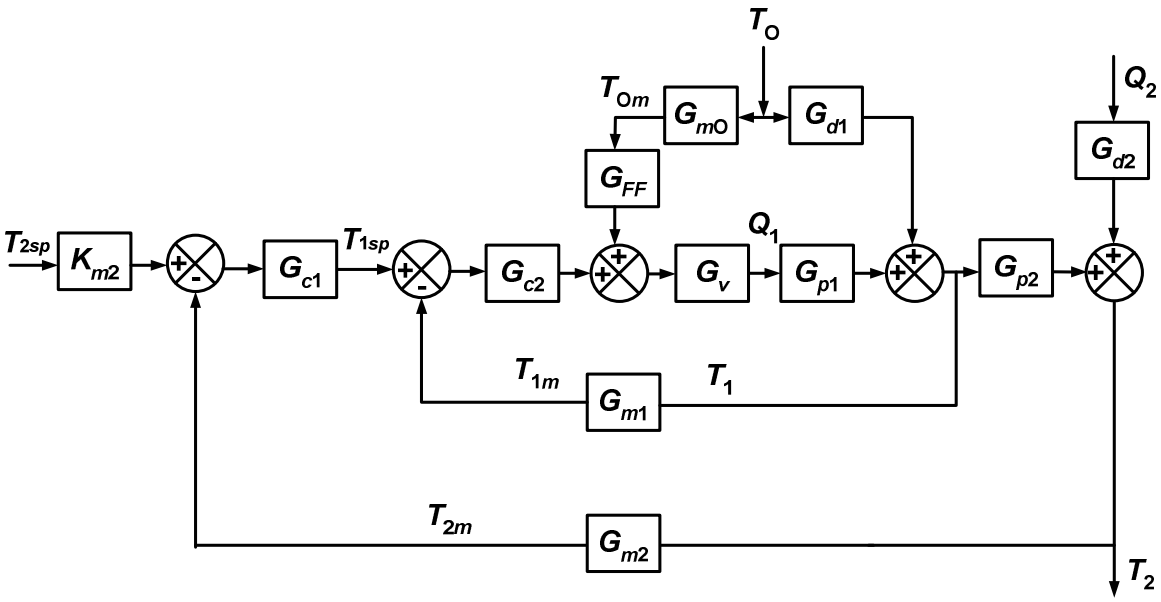

Figure S16.5b. *Block diagram for the control system in Exercise 16.5.*

16.6

a) For the inner loop, the characteristic equation reduces to:

$$1 + K_{inner}\,\frac{s+1}{s-3} = 0 \quad \because \quad s - 3 + K_{inner}\,s + K_{inner} = 0$$

$$\because \quad s(1+K_{inner}) - 3 + K_{inner} = 0$$

Hence, $s = \dfrac{3 - K_{inner}}{1 + K_{inner}}$

The inner loop will be stable if this root is negative. Thus, we conclude that this loop will be stable if either $K_{inner}>3$ or $K_{inner}<-1$.

b) The servo transfer function for the outer loop is:

$$\frac{Y(s)}{Y_{sp}(s)} = \frac{G_c(s)\,K_{inner}\,G_p(s)}{1 + K_{inner}G_p(s) + G_c(s)K_{inner}G_p(s)}$$

The complex closed-loop poles arise when the characteristic polynomial is factored. This polynomial is

$$(s^2 + s + 0.313) = (s + 0.5 + 0.25\,i)\,(s + 0.5 - 0.25\mathrm{i})$$

$$1 + 6\frac{s+1}{s-3} + K_c\left(\frac{\tau_I s + 1}{\tau_I s}\right)6\frac{s+1}{s-3} = 0$$

$$\because \left(\tau_I + 6\tau_I + K_c 6\tau_I\right)s^2$$

$$+(-3\tau_I + 6\tau_I + 6\tau_I K_c + 6K_c)s$$

$$+ K_c 6 = 0$$

The poles are also the roots of the characteristic equation:

Hence, the PI controller parameters can be found easily:

$$K_c = 0.052$$

$$\tau_I = 0.137$$

16.7

Using MATLAB-Simulink, the block diagram for the closed-loop system is shown below.

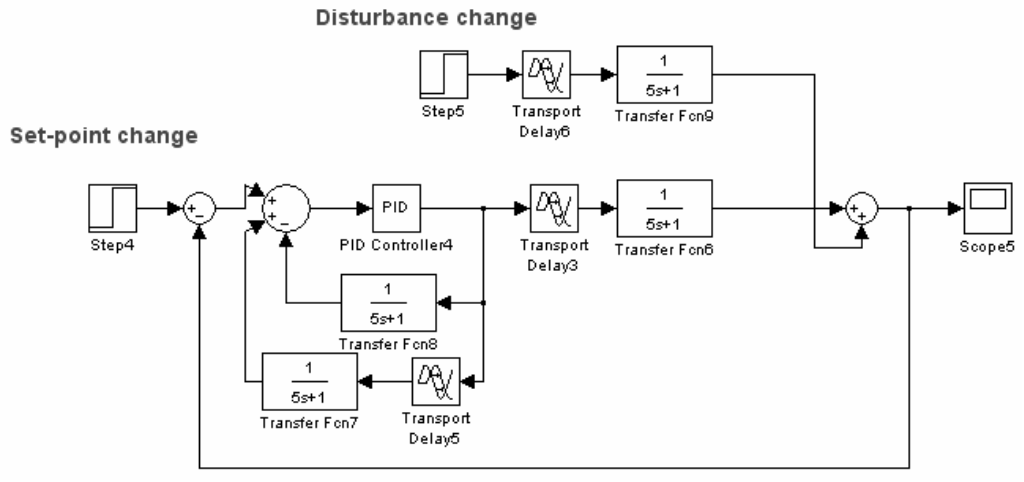

Figure S16.7a. *Block diagram for Smith predictor*

where the block  represents the time-delay term $e^{-\theta s}$.

The closed-loop response for unit set-point and disturbance changes are shown below. Consider a PI controller designed by using Table 12.1(Case A) with $\tau_c = 3$ and set $G_d = G_p$. Note that no offset occurs,

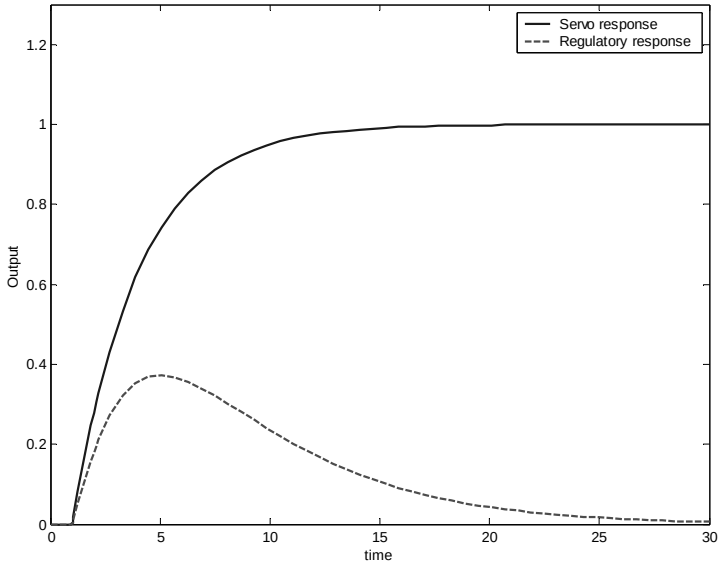

Figure S16.7b. *Closed-loop response for setpoint and disturbance changes.*

16.8

The block diagram for the closed-loop system is

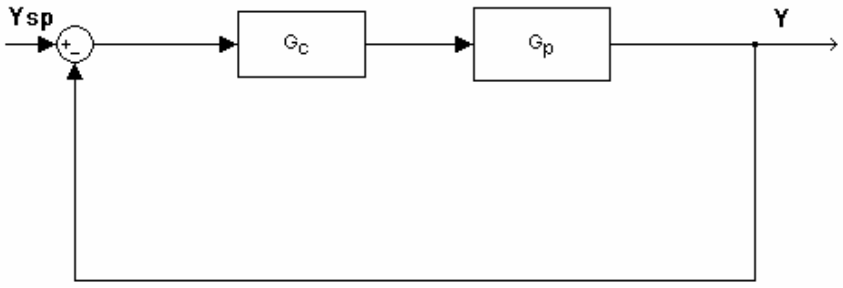

Figure S6.8. *Block diagram for the closed-loop system*

where $G_c = K_c\left(\dfrac{1+\tau_I s}{1+\tau_I s - e^{-\theta s}}\right)$ *and* $G_p = \dfrac{K_p e^{-\theta s}}{1+\tau s}$

a)

$$\frac{Y}{Y_{sp}} = \frac{G_c G_p}{1 + G_c G_p} = \frac{K_c K_p \left(\frac{1 + \tau_I s}{1 + \tau_I s - e^{-\theta s}} \right) \frac{e^{-\theta s}}{1 + \tau s}}{1 + K_c K_p \left(\frac{1 + \tau_I s}{1 + \tau_I s - e^{-\theta s}} \right) \frac{e^{-\theta s}}{1 + \tau s}}$$

Since $K_c = \frac{1}{K_p}$ and $\tau_I = \tau$

$$\frac{Y}{Y_{sp}} = \frac{\left(\frac{e^{-\theta s}}{1 + \tau_I s - e^{-\theta s}} \right)}{1 + \left(\frac{e^{-\theta s}}{1 + \tau_I s - e^{-\theta s}} \right)} = \frac{e^{-\theta s}}{1 + \tau_I s - e^{-\theta s} + e^{-\theta s}}$$

Hence dead-time is eliminated from characteristic equation:

$$\frac{Y}{Y_{sp}} = \frac{e^{-\theta s}}{1 + \tau_I s}$$

b) The closed-loop response will not exhibit overshoot, because it is a first order plus dead-time transfer function.

16.9

For a first-order process with time delay, use of a Smith predictor and proportional control should make the process behave like a first-order system, i.e., no oscillation. In fact, if the model parameters are accurately known, the controller gain can be as large as we want, and no oscillations will occur.

Appelpolscher has verified that the process is linear, however it may not be truly first-order. If it were second-order (plus time delay), proportional control would yield oscillations for a well-tuned system. Similarly, if there are errors in the model parameters used to design the controller even when the actual process is first-order, oscillations can occur.

16.10

a) Analyzing the block diagram of the Smith predictor

$$\frac{Y}{Y_{sp}} = \frac{G_c G_p' e^{-\theta s}}{1 + G_c \tilde{G}_p' (1 - e^{-\tilde{\theta} s}) + G_c G_p' e^{-\theta s}}$$

$$= \frac{G_c G_p' e^{-\theta s}}{1 + G_c \tilde{G}_p' + G_c G_p' e^{-\theta s} - G_c \tilde{G}_p' e^{-\tilde{\theta} s}}$$

Note that the last two terms of the denominator can when $G_p' = \tilde{G}_p'$ and $\theta = \tilde{\theta}$

The characteristic equation is

$$= 1 + G_c \tilde{G}_p' + G_c G_p' e^{-\theta s} - G_c \tilde{G}_p' e^{-\tilde{\theta} s} = 0$$

b) The closed-loop responses to step set-point changes are shown below for the various cases.

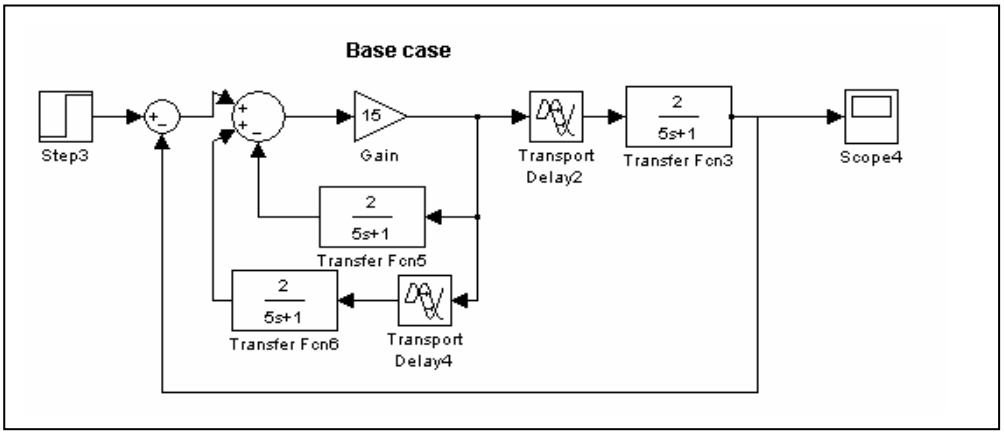

Figure S16.10a. *Simulink diagram block; base case*

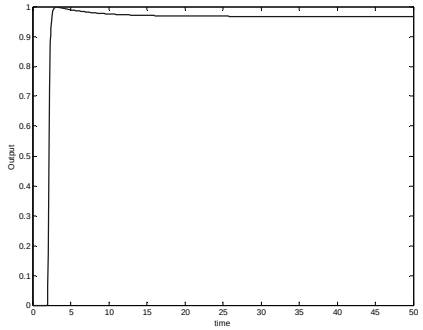

Figure S16.10b. *Base case*

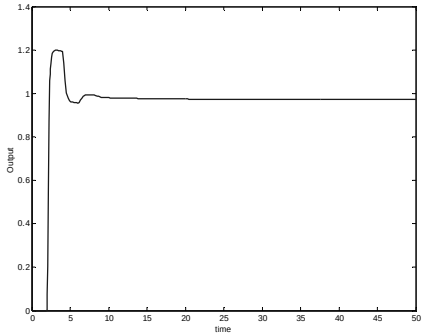

Figure S16.10c. $K_p = 2.4$

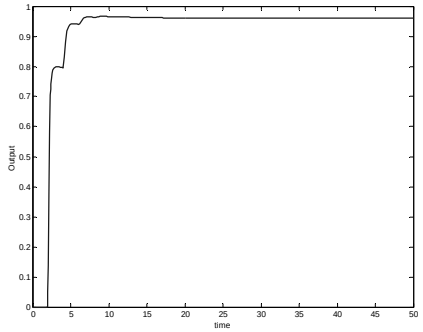

Figure S16.10d. $K_p = 1.6$

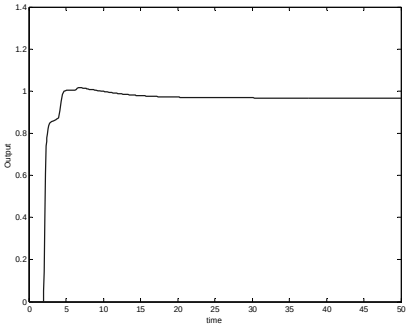

Figure S16.10e. $\tau = 6$

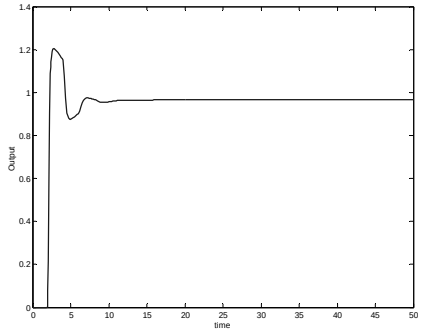

Figure S16.10f. $\tau = 4$

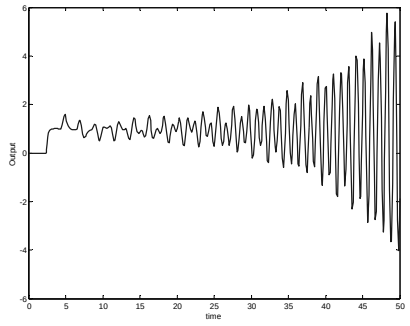

Figure S16.10g. $\theta=2.4$

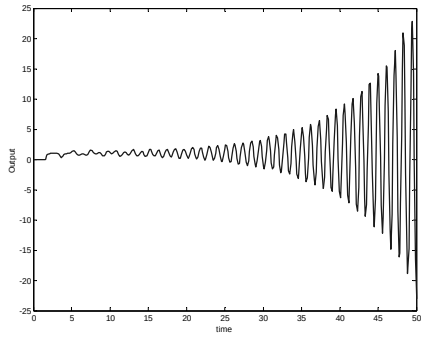

Figure S16.10h. $\theta = 1.6$

It is immediately evident that errors in time-delay estimation are the most serious. This is because the terms in the characteristic equation which contain dead-time do not cancel, and cause instability at high controller gains.

When the actual process time constant is smaller than the model time constant, the closed–loop system may become unstable. In our case, the error is not large enough to cause instability, but the response is more oscillatory than for the base (perfect model) case. The same is true if the actual process gain is larger than that of the model. If the actual process has a larger time constant, or smaller gain than the model, there is no significant degradation in closed loop performance (for the magnitude of the error, ± 20% considered here). Note that in all the above simulations, the model is considered to be $\frac{2e^{-2s}}{5s+1}$ and the actual process parameters have been assumed to vary by ± 20% of the model parameter values.

c) The proportional controller was tuned so as to obtain a gain margin of 2.0. This resulted in K_c = 2.3. The responses for the various cases are shown below

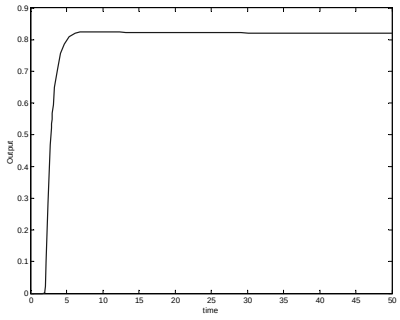

Base case

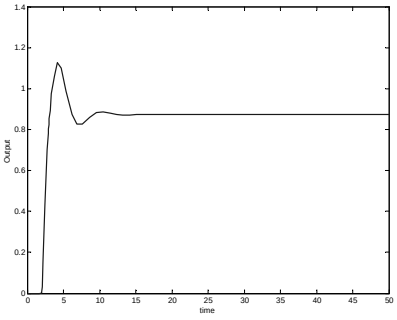

K_p = 3

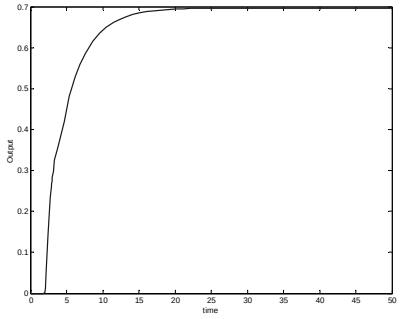

$K_p = 1$

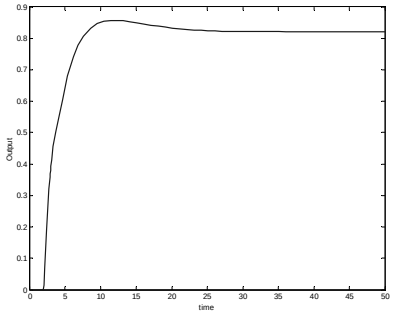

$\tau = 1$

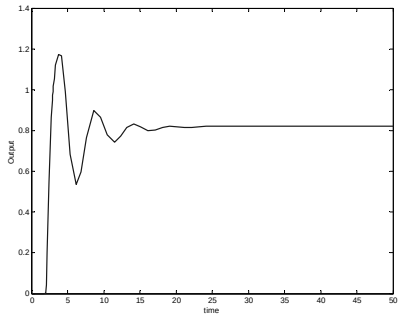

$\tau = 2.5$

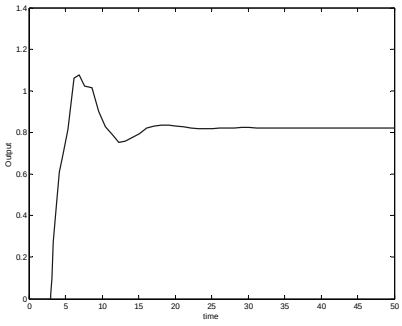

$\theta = 3$

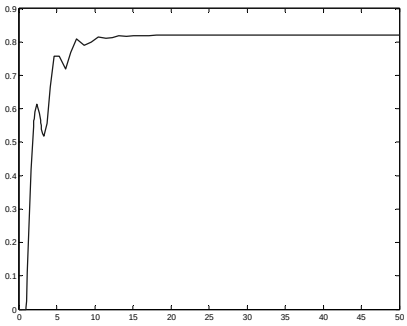

$\theta = 1$

Nyquist plots were prepared for different values of K_p, τ and θ, and checked to see if the stability criterion was satisfied. The stability regions when the three parameters are varied one to time are.

$K_p \leq 4.1 \quad (\tau = 5 \quad , \quad \theta = 2)$

$\tau \quad \geq 2.4 \quad (K_p = 2 \quad , \quad \theta = 2)$

$\theta \quad \leq 0.1 \quad \text{and } 1.8 \leq \theta \leq 2.2 \quad (K_p = 2 \quad , \quad \tau = 5)$

16.11

From Eq. 16-24,

$$\frac{Y}{D} = \frac{G_d\left(1+G_cG^*\left(1-e^{-\theta s}\right)\right)}{1+G_cG^*}$$

that is,

$$\frac{Y}{D} = \frac{\frac{2}{s}e^{-3s}\left(1+\frac{K_c+K_c\tau_I s}{\tau_I s}\frac{2}{s}\left(1-e^{-3s}\right)\right)}{1+\frac{K_c+K_c\tau_I s}{\tau_I s}\frac{2}{s}}$$

Using the final value theorem for a step change in D:

$$\lim_{t\to\infty} y(t) = \lim_{s\to 0} sY(s)$$

then

$$\lim_{s\to 0} sY(s) = \lim_{s\to 0}\ s\ \frac{\frac{2}{s}e^{-3s}\left(1+\frac{K_c+K_c\tau_I s}{\tau_I s}\frac{2}{s}\left(1-e^{-3s}\right)\right)}{1+\frac{K_c+K_c\tau_I s}{\tau_I s}\frac{2}{s}}\frac{1}{s}$$

$$= \lim_{s\to 0}\ \frac{\frac{2}{s}e^{-3s}\left(\tau_I s+(K_c+K_c\tau_I s)\frac{2}{s}\left(1-e^{-3s}\right)\right)}{\tau_I s+(K_c+K_c\tau_I s)\frac{2}{s}}$$

Multiplying both numerator and denominator by s^2,

$$= \lim_{s\to 0}\ \frac{2e^{-3s}\left(\tau_I s^2+(K_c+K_c\tau_I s)2\left(1-e^{-3s}\right)\right)}{\tau_I s^3+(K_c+K_c\tau_I s)2s}$$

Applying L'Hopital's rule:

$$= \lim_{s\to 0}\ \frac{-6e^{-3s}\left(\tau_I s^2+(K_c+K_c\tau_I s)2\left(1-e^{-3s}\right)\right)}{3\tau_I s^2+2(K_c+2K_c\tau_I s)}$$

$$+\ \frac{2e^{-3s}(2\tau_I s+6K_ce^{-3s}+2K_c\tau_I-2K_c\tau_Ie^{-3s}+6K_c\tau_Ise^{-3s})}{3\tau_I s^2+2(K_c+2K_c\tau_I s)}\ =\ 6$$

Therefore

$$\lim_{t\to\infty} y(t) = \lim_{s\to 0} sY(s) = 6$$

and the PI control will not eliminate offset.

16.12

For a Smith predictor, we have the following system

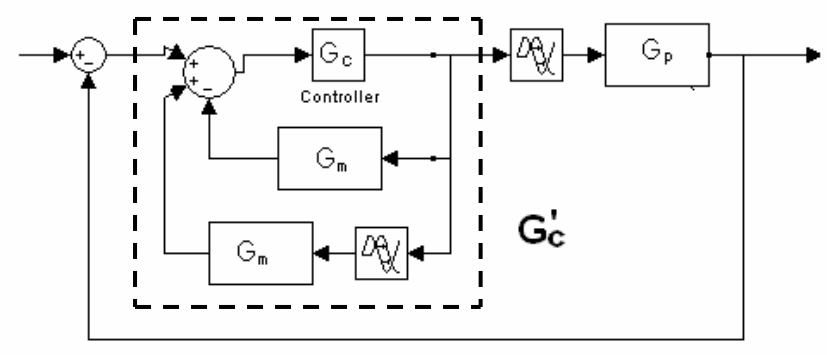

Figure S16.12. *Smith Predictor diagram block*

where the process model is $G_p(s) = Q(s)\, e^{-\theta s}$

For this system,

$$\frac{Y}{Y_{sp}} = \frac{G_c' G_p}{1 + G_c' G_p}$$

where G_c' is the transfer function for the system in the dotted box.

$$G_c' = \frac{G_c}{1 + G_c Q(1 - e^{-\theta s})}$$

$$\therefore \frac{Y}{Y_{sp}} = \frac{\dfrac{G_c G_p}{1 + G_c Q(1 - e^{-\theta s})}}{1 + \dfrac{G_c G_p}{1 + G_c Q(1 - e^{-\theta s})}}$$

Simplification gives

$$\frac{Y}{Y_{sp}} = \frac{G_c Q e^{-\theta s}}{1 + G_c Q} = P(s) e^{-\theta s}$$

where $P(s) = \dfrac{G_c Q}{1 + G_c Q}$

If $P(s)$ is the desired system performance (after the time delay has elapsed) under feedback control, then we can solve for G_c in terms of $P(s)$.

$$G_c = \frac{P(s)}{Q(s)(1 - P(s))}$$

The IMC controller requires that we define

$$\tilde{G}_+ = e^{-\theta s}$$

$$\tilde{\tilde{G}}_- = Q(s) \qquad \text{(the invertible part of } G_p\text{)}$$

Let the filter for the controller be $f(s) = \dfrac{1}{\tau_F s + 1}$

Therefore, the controller is

$$G_c = \tilde{\tilde{G}}_-^{-1} f(s) = \frac{f(s)}{Q(s)}$$

The closed-loop transfer function is

$$\frac{Y}{Y_{sp}} = G_c G_p = \frac{e^{-\theta s}}{1 + \tau_F s} = \tilde{G}_+ f$$

Note that this is the same closed-loop form as analyzed in part (a), which led to a Smith Predictor type of controller. Hence, the IMC design also provides time-delay compensation.

16.13

Referring to Example 4.8, if q, the flowrate, and T_i, the inlet temperature, are know and are constant, then the Laplace transform models in (4-79) and (4-80) are

$$(s - a_{11})C_A'(s) = a_{12}T'(s) \tag{4-79}$$

$$(s - a_{22})T'(s) = a_{12}C_A'(s) + b_2T_s'(s) \tag{4-80}$$

where $T_s'(s)$ is the coolant temperature. Using Eq. 4-86, we can directly compute concentration from the temperature signal, i.e.,

$$C_A'(s) = \frac{a_{12}}{s - a_{11}}T'(s)$$

which is a first-order filter operating on $T'(s)$

So inferential control of concentration using temperature would be feasible in this case. If q and T_i varied, a more general expression for the linearized model would be necessary, but there would still be a direct way to infer C_A from T.

16.14

One possible solution would be to use a split range valve to handle the $100 \leq p \leq 200$ and higher pressure ranges. Moreover, a high-gain controller with set-point = 200 psi can be used for the vent valve. This valve would not open while the pressure is less than 200 psi, which is similar to how a selector operates.

Stephanopoulos (Chemical Process Control, Prentice-Hall, 1989) has described many applications for this so-called split-range control. A typical configuration consists of 1 controller and 2 final control elements or valves.

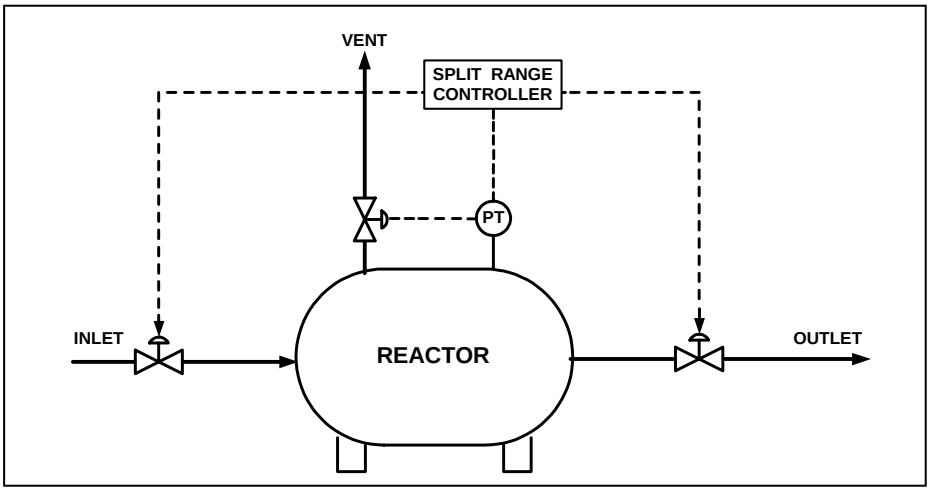

Figure S16.14. *Process instrumentation diagram*

16.15

The amounts of air and fuel are changed in response to the steam pressure. If the steam pressure is too low, a signal is sent to increase both air and fuel flowrates, which in turn increases the heat transfer to the steam. Selectors are used to prevent the possibility of explosions (low air-fuel ratio). If the air flowrate is too low, the low selector uses that measurement as the set-point for the fuel flow rate controller. If the fuel flowrate is too high, its measurement is selected by the high selector as the set-point for the air flow controller. This also protects against dynamic lags in the set-point response.

16.16

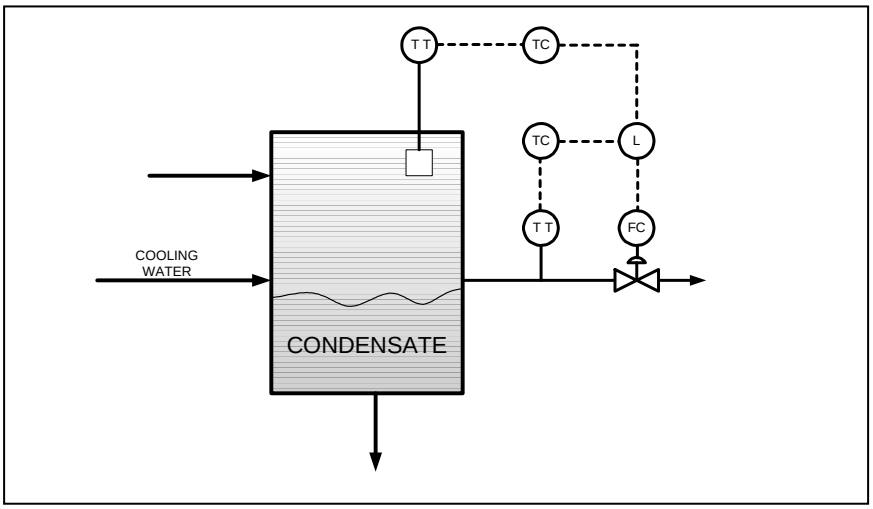

Figure S16.16. *Control condensate temperature in a reflux drum*

16.17

Supposing a first-order plus dead time process, the closed-loop transfer function is

$$G_{CL}(s) = \frac{G_c G_p}{1 + G_c G_p} \quad \therefore \quad G_{CL}(s) = \frac{K_c K_p \dfrac{\left(1 + \dfrac{1}{\tau_I s} + \tau_D s\right) e^{-\theta s}}{(\tau_p s + 1)}}{1 + K_c K_p \dfrac{\left(1 + \dfrac{1}{\tau_I s} + \tau_D s\right) e^{-\theta s}}{(\tau_p s + 1)}}$$

Notice that K_c and K_p always appear together as a product. Hence, if we want the process to maintain a specified performance (stability, decay ratio specification, etc.), we should adjust K_c such that it changes inversely with K_p; as a result, the product $K_c K_p$ is kept constant. Also note, that since there is a time delay, we should adjust K_c based upon the future estimate of K_p:

$$K_c(t) = \frac{\bar{K}_c \bar{K}_p}{\hat{K}_p(t + \theta)} = \frac{\bar{K}_c \bar{K}_p}{a + \dfrac{b}{\hat{M}(t + \theta)}}$$

where $\hat{K}_p(t + \theta)$ is an estimate of K_p θ time units into the future.

16.18

This is an application where self-tuning control would be beneficial. In order to regulate the exit composition, the manipulated variable (flowrate) must be adjusted. Therefore, a transfer function model relating flowrate to exit composition is needed. The model parameters will change as the catalyst deactivates, so some method of updating the model (e.g., periodic step tests) will have to be derived. The average temperature can be monitored to determine a significant change in activation has occurred, thus indicating the need to update the model.

16.19

a) $$\frac{G_c G_p}{1+G_c G_p} = \frac{1}{\tau_c s+1} \quad \therefore \quad G_c = \frac{\dfrac{1}{\tau_c s+1}}{G_p\left(1-\dfrac{1}{\tau_c s+1}\right)} = \frac{1}{G_p}\frac{1}{\tau_c s}$$

Substituting for G_p

$$G_c(s) = \frac{1}{\tau_c s}\frac{\tau_1\tau_2 s^2+(\tau_1+\tau_2)s+1}{K_p} = \frac{1}{K_p\tau_c}\left[(\tau_1+\tau_2)+\tau_1\tau_2 s+\frac{1}{s}\right]$$

Thus, the PID controller tuning constants are

$$K_c = \frac{(\tau_1+\tau_2)}{K_p\tau_c}$$

$$\tau_I = \tau_1+\tau_2$$

$$\tau_D = \frac{\tau_1\tau_2}{\tau_1+\tau_2}$$

(See Eq. 12-14 for verification)

b) For $\tau_1 = 3$ and $\tau_2 = 5$ and $\tau_c = 1.5$, we have

$K_c = 5.333$ $\tau_I = 8.0$ and $\tau_D = 1.875$

Using this PID controller, the closed-loop response will be first order when the process model is known accurately. The closed-loop response to a unit step-change in the set-point when the model is known exactly is shown above. It is assumed that τ_c was chosen such that the closed loop response is reasonable, and the manipulated variable does not violate any bounds that are imposed. An approximate derivative action is used by Simulink-MATLAB, namely $\dfrac{\tau_D s}{1+\beta s}$ when β=0.01

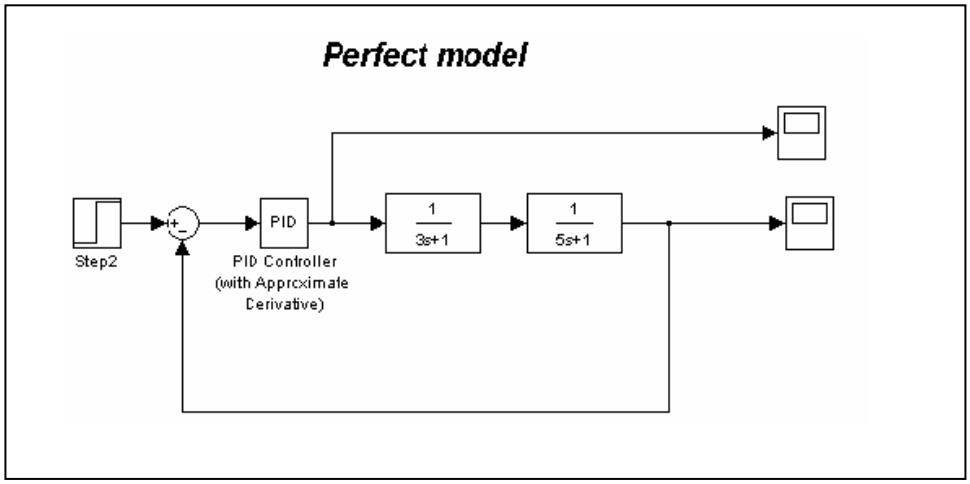

Figure S16.19a. *Simulink block diagram.*

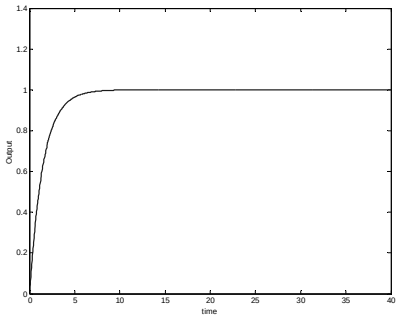

Figure S16.19b. *Output (no model error)*

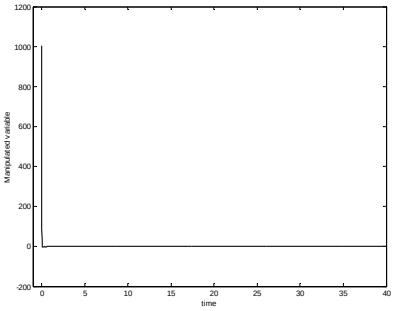

Figure S16.19c. *Manipulated variable (no model error)*

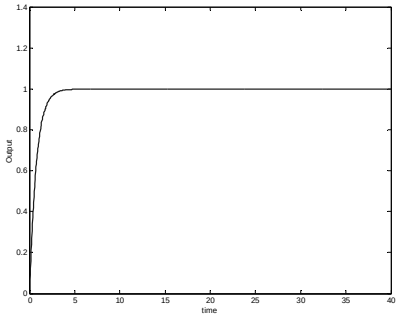

Figure S16.19d. *Output (K_p = 2)*

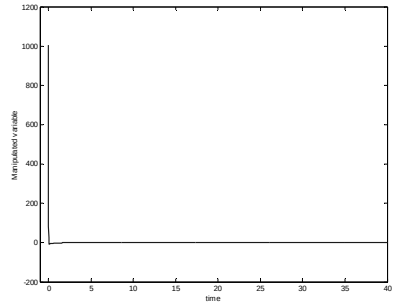

Figure S16.19e. *Manipulated variable (K_p = 2)*

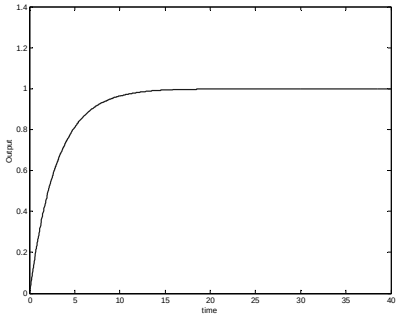

Figure S16.19f. *Output (K_p = 0.5)*

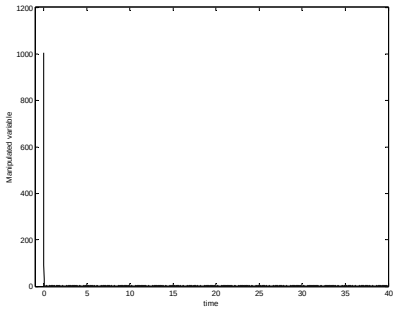

Figure S16.19g. *Manipulated variable (K_p =0.5)*

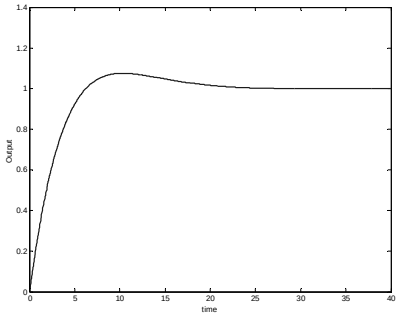

Figure S16.19h. *Output (τ_2 = 10)*

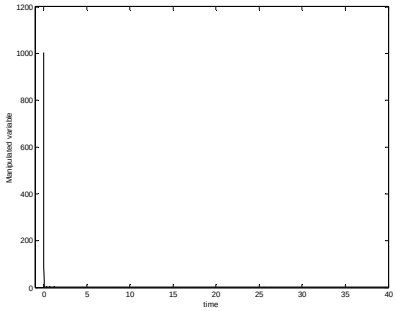

Figure S16.19i. *Manipulated variable (τ_2 = 10)*

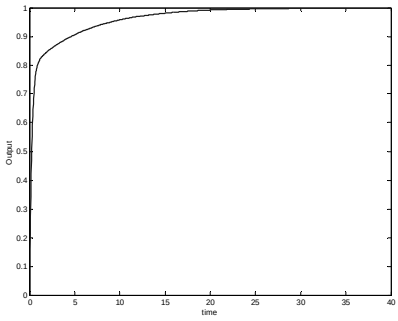

Figure E16.9 j.- *Output (τ_2 = 1)*

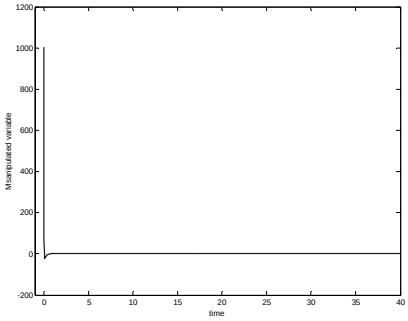

Figure E16.9 k.- *Manipulated variable (τ_2 = 1)*

(1) The closed-loop response when the actual K_p is 2.0 is shown above. The controlled variable reaches its set-point much faster than for the base case (exact model), but the manipulated variable assumes values that are more negative (for some period of time) than the base case. This may violate some bounds.

(2) When $K_p = 0.5$, the response is much slower. In fact, the closed-loop time constant seems to be about 3.0 instead of 1.5. There do not seem to be any problems with the manipulated variable.

(3) If ($\tau_2 = 10$), the closed-loop response is no longer first-order. The settling time is much longer than for the base case. The manipulated variable does not seem to violate any bounds.

(4) Both the drawbacks seen above are observed when $\tau_2 = 1$. The settling time is much longer than for the base case. Also the rapid initial increase in the controlled variable means that the manipulated variable drops off sharply, and is in danger of violating a lower bound.

16.20

Based on discussions in Chapter 12, increasing the gain of a controller makes it more oscillatory, increasing the overshoot (peak error) as well as the decay ratio. Therefore, if the quarter-decay ratio is a goal for the closed-loop response (e.g., Ziegler-Nichols tuning), then the rule proposed by Appelpolscher should be satisfactory from a qualitative point of view. However, if the controller gain is increased, the settling time is also decreased, as is the period of oscillation. Integral action influences the response characteristics as well. In general, a decrease in τ_I gives comparable results to an increase in K_c. So, K_c can be used to influence the peak error or decay ratio, while τ_I can be used to speed up the settling time (a decrease in τ_I decreases the settling time). See Chapter 8 for typical response for varying K_c and τ_I.

16.21

SELECTIVE CONTROL

Selectors are quite often used in forced draft combustion control system to prevent an imbalance between air flow and fuel flow, which could result in unsafe operating conditions.

For this case, a flow controller adjusts the air flowrate in the heater. Its set-point is determined by the High Selector, which chooses the higher of the two input signals:

.- Signal from the fuel gas flowrate transmitter (when this is too high)

.- Signal from the outlet temperature control system.

Similarly, if the air flow rate is too low, its measurement is selected by the low selector as the set-point for the fuel-flow rate.

CASCADE CONTROLLER

The outlet temperature control system can be considered the master controller that adjusts the set-point of the fuel/air control system (slave controller). If a disturbance in fuel or air flow rate exists, the slave control system will act very quickly to hold them at their set-points.

FEED-FORWARD CONTROL

The feedforward control scheme in the heater provides better control of the heater outlet temperature. The feed flowrate and temperature are measured and sent to the feedback control system in the outflow. Hence corrective action is taken before they upset the process. The outputs of the feedforward and feedback controller are added together and the combined signal is sent to the fuel/air control system.

16.22

ALTERNATIVE A.-

Since the control valves are "air to close", each K_v is positive (cf. Chapter 9). Consequently, each controller must be reverse acting (K_c>0) for the flow control loop to function properly.

Two alternative control strategies are considered:

Method 1: use a default feed flowrate when $P_{cc} > 80\%$

Let : P_{cc} = output signal from the composition controller (%)
$\tilde{F}_{sp}$ = (internal) set point for the feed flow controller (%)

Control strategy:

If $P_{cc} > 80\%$, $\tilde{F}_{sp} = \tilde{F}_{sp,low}$

where $\tilde{F}_{sp,low}$ is a specified default flow rate that is lower than the normal value, $\tilde{F}_{sp\,nom}$.

Method 2: Reduce the feed flow when $P_{cc} > 80\%$

Control strategy:

$$\text{If } P_{cc} < 80\%, \quad \tilde{\tilde{F}}_{sp} = \tilde{\tilde{F}}_{sp\,nom} - K(P_{cc} - 80\%)$$

where K is a tuning parameter ($K > 0$)

Implementation:

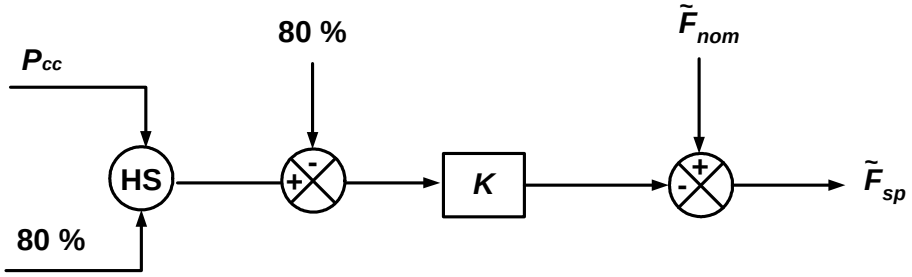

Note: A check should be made to ensure that $0 \le \tilde{\tilde{F}}_{sp} \le 100\%$

ALTERNATIVE B.-

A selective control system is proposed:

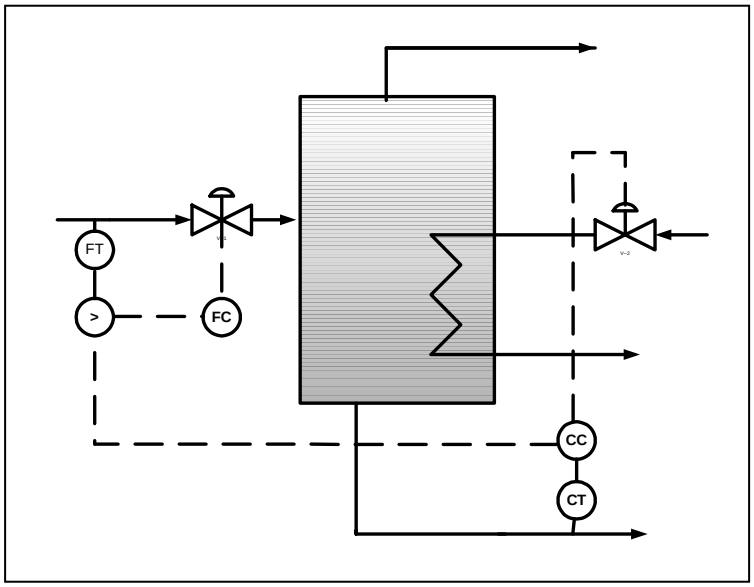

Figure S16.22. *Proposed selective control system*

Both control valves are A-O and transmitters are "direct acting", so the controller have to be "reverse acting".

When the output concentration decreases, the controller output increases. Hence this signal cannot be sent directly to the feed valve (it would open

the valve). Using a high selector that chooses the higher of these signals can solve the problem

.- Flow transmitter
.- Output concentration controller

Therefore when the signal from the output controller exceeds 80%, the selector holds it and sends it to the flow controller, so that feed flow rate is reduced.

16.23

ALTERNATIVE A.-

Time delay.- Use time delay compensation, e.g., Smith Predictor

Variable waste concentration.- Tank pH changes occurs due to this unpredictable changes. Process gain changes also (c,f. literature curve for strong acid-strong base)

Variable waste flow rate.- Use FF control or ratio q_{base} to q_{waste}.

Measure q_{base} .- This suggests you may want to use cascade control to compensate for upstream pressure changes, etc

ALTERNATIVE B.-

Several advanced control strategies could provide improved process control. A selective control system is commonly used to control pH in wastewater treatment .The proposed system is shown below (pH T = pH sensor; pH C = pH controller)

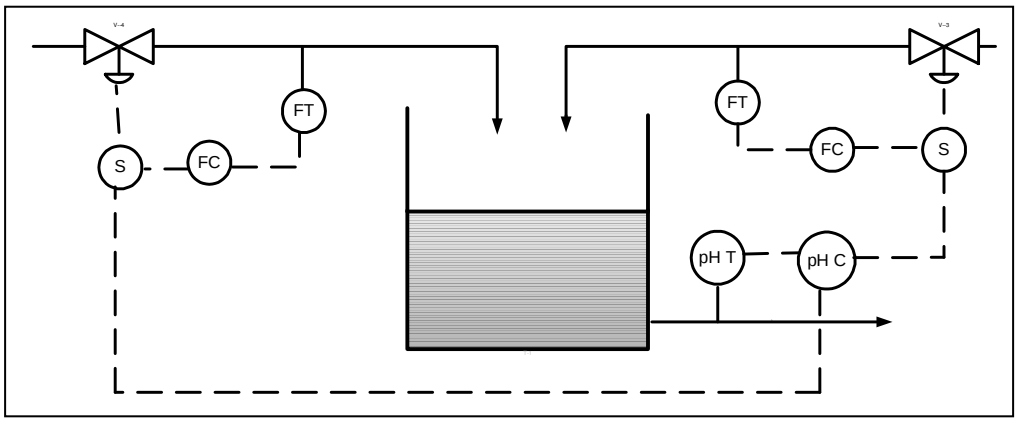

Figure S16.23. *Proposed selective control system.*

where S represents a selector (< or > , to be determined)

In this scheme, several manipulated variables are used to control a single process variable. When the pH is too high or too low, a signal is sent to the selectors in either the waste stream or the base stream flowrate controllers. The exactly configuration of the system depends on the transmitter, controller and valve gains.

In addition, a Smith Predictor for the pH controller is proposed due to the large time delay. There would be other possibilities for this process such as an adaptive control system or a cascade control system. However the scheme above may be good enough

Necessary information:

.- Descriptions of measurement devices, valves and controllers; direct action or reverse action.

.- Model of the process in order to implement the Smith Predictor

16.24

For setpoint change, the closed-loop transfer function with an integral controller and steady state process ($G_p = K_p$) is:

$$\frac{Y}{Y_{sp}} = \frac{G_C G_P}{1 + G_C G_P} = \frac{\frac{1}{\tau_I s} K_P}{1 + \frac{1}{\tau_I s} K_P} = \frac{K_P}{\tau_I s + K_P} = \frac{1}{\frac{\tau_I}{K_P} s + 1}$$

Hence a first order response is obtained and satisfactory control can be achieved.

For disturbance change ($G_d = G_p$):

$$\frac{Y}{D} = \frac{G_d}{1 + G_C G_P} = \frac{K_P}{1 + \frac{1}{\tau_I s} K_P} = \frac{K_P(\tau_I s)}{\tau_I s + K_P} = \frac{\tau_I s}{\frac{\tau_I}{K_P} s + 1}$$

Therefore a first order response is also obtained for disturbance change.